Role of *A*-site cations in the metal-insulator transition in $Pr_{0.5}Ca_{0.5}CoO_{3-\gamma}$ ($\gamma \approx 0$)

A. J. Barón-González,[1] C. Frontera,[1] J. L. García-Muñoz,[1] J. Blasco,[2] and C. Ritter[3]
[1]*Institut de Ciència de Materials de Barcelona-CSIC, Campus Universitari de Bellaterra, 08193 Bellaterra, Spain*
[2]*Instituto de Ciencias de Materiales de Aragón, Departamento de Física de la Materia Condensada, CSIC–Universidad de Zaragoza, c/Pedro Cerbuna 12, 50009 Zaragoza, Spain*
[3]*Institut Laue Langevin, 6 rue Jules Horowitz, 38100 Grenoble, France*
(Received 13 May 2009; revised manuscript received 9 October 2009; published 18 February 2010)

Remarkable structural changes take place during the metal to insulator first-order transition in $Pr_{0.50}Ca_{0.50}CoO_3$: a contraction of the unit-cell volume, the bending of the Co-O-Co bond angle, and a decrease in (Pr,Ca)-O bond distance. However, the Co-O bond length and the volume of the CoO_6 octahedra remain almost unaltered during the transition. In view of these data and the absence of transition in $(Nd_{2/3}La_{1/3})_{0.5}Ca_{0.5}CoO_3$, we review the current spin-state transition picture, emphasizing that an active role is played by the *A*-site Pr cations that could be related with the effect of Pr in 123 superconducting cuprates.

DOI: 10.1103/PhysRevB.81.054427 PACS number(s): 71.30.+h, 61.05.fm, 75.30.Kz, 75.47.De

I. INTRODUCTION

Cobalt oxides are attracting a growing interest for several different reasons. From an applied point of view, different cobalt compounds present interesting features in different applications as mixed conductors, materials for solid oxides fuel cells, thermopower applications, room-temperature (RT) ferromagnets, or magnetodielectric materials.[1–4] From a fundamental point of view, these oxides present complex behavior, magnetoresistance, intriguing metal-insulator transitions, superconductivity, spin-state transitions, charge order, etc.[5–12] The ability of cobalt ions in perovskite structure to present different spin states as a function of temperature, applied field, pressure, chemical tuning, etc., plays a major role in this richness.

The spin state of cobalt has been reported to vary smoothly with temperature in $LaCoO_3$ signaling that the transition between low spin (LS with $S=0$ and t_{2g}^6) and higher spin states (intermediate spin, IS, with $S=1$, $t_{2g}^5e_g^1$; and high spin, HS, with $S=2$, $t_{2g}^4e_g^2$) takes place by thermal activation.[9,10] Besides, other Co oxides, such as $RBaCo_2O_{5.50}$ family (R=rare earth, Y) present a sudden change between two different spin states at a well-defined temperature that is linked to a metal (higher spin) to insulator (lower spin) transition.[11]

In both mentioned examples ($RCoO_3$ and $RBaCo_2O_{5.50}$), the change in the spin state is accompanied by changes in the unit-cell volume (V), which expands when the Co spin increases.[10,11] In the first case, there is an anomalous term in the dependence on temperature of V while in the second, the change is sudden (as the spin-state transition). These variations in V are driven by a significant modification of Co-O bond distances. The population of e_g orbitals to give IS and/or HS states in CoO_6 octahedra are favored by weak crystal fields (large Co-O bond distances) and straight Co-O-Co angles.[13] Beside these examples, layered cobaltites such as $Pr_{2-x}Ca_xCoO_4$ ($x \sim 0.5$) and $La_{1.5}Sr_{0.5}CoO_4$ present a charge-ordering (CO) transition with increasing electron localization related with a spin-state change.[12] In $Pr_{2-x}Ca_xCoO_4$, the spin-state change occurs near half doping when changing x but CO takes place independently. Polaronic superlattice correlations originating from electron-electron and electron-lattice interactions were identified as drivers of the CO transition.

Another example where a sudden spin-state transition has been claimed is $Pr_{0.50}Ca_{0.50}CoO_3$.[14–22] This compound presents, on cooling a sudden increase in the resistivity, usually described as a metal to insulator transition (MIT). It is accompanied by an anisotropic cell anomaly and a sudden large cell volume contraction. This MIT has been interpreted as the sudden formation of mixed localized Co^{3+} and Co^{4+} ($S=\frac{1}{2}$, t_{2g}^5) LS states whereas above T_{MI}, a delocalized homogeneous $t_{2g}^5(\sigma^*)^{0.5}$ state would be responsible for carrier conduction (as reported earlier for $Pr_{0.50}Sr_{0.50}CoO_3$).

For the sake of comparison, it is worth to recall that $Pr_{0.50}Sr_{0.50}CoO_3$ presents a ferromagnetic (FM) and metallic ground state. Ferromagnetism disappears above $T_C=225$ K and metallicity extends well above this temperature.[23] Double exchange is thought to contribute to the ferromagnetic interaction leading to a peak in the magnetoresistance at T_C. Different authors have reported a similar behavior (ferromagnetic at low T and conducting over a wide temperature range) for $R_{0.50}Sr_{0.50}CoO_3$ with R=La, Nd, Sm, and Eu.[24–26]

In this paper, we present the results of a detailed structural study of $Pr_{0.50}Ca_{0.50}CoO_3$ as a function of temperature that allows us to monitor the changes across the transition. The atomic shifts producing the sharp volume contraction at the transition are quite unusual in perovskites. These structural results are accompanied by resistivity, magnetotransport, and magnetic studies that allow us to make a critical review of the picture described above. The behavior observed is not compatible with the simple picture of a spin-state transition and evidence that Pr ions play a key role in the transition. An independent corroboration of these conclusions is obtained by confirming the absence of this transition in $La_{1/6}Nd_{1/3}Ca_{0.5}CoO_3$ (without Pr but with identical doping and average ionic radius at A site).

II. EXPERIMENTAL DETAILS

Polycrystalline samples ($Pr_{0.50}Ca_{0.50}CoO_3$ and $La_{1/6}Nd_{1/3}Ca_{0.5}CoO_3$) have been prepared by solid-state re-

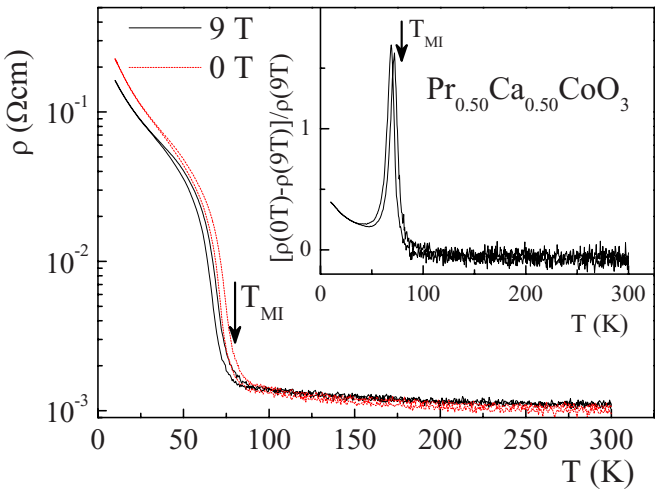

FIG. 1. (Color online) Variation under temperature of the four-probe resistivity of $Pr_{0.50}Ca_{0.50}CoO_3$ without applied field and under an applied field of 9 T. Measures have been done following a cooling-heating cycle. The inset shows the magnetoresistance.

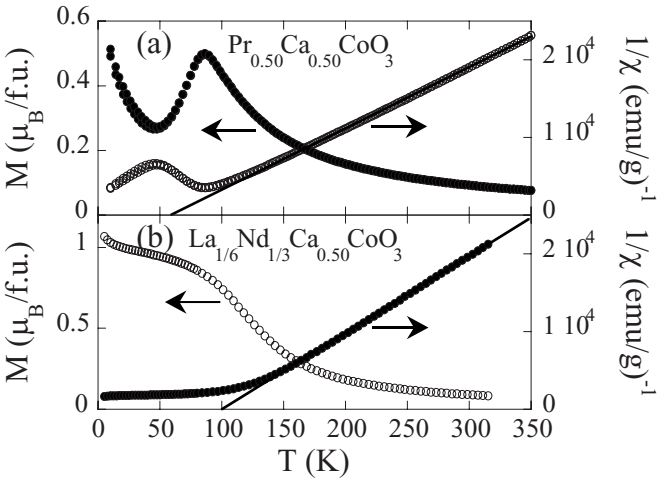

FIG. 2. Temperature dependence of the magnetization (left axis) and inverse susceptibility (right axis) of (a) $Pr_{0.50}Ca_{0.50}CoO_3$ and (b) $La_{1/6}Nd_{1/3}Ca_{0.5}CoO_3$ measured under 5 T on heating after zero-field cooling and field cooling.

action in air. Stoichiometric fractions of high-purity Pr_6O_{11}, La_2O_3, Nd_2O_3, Co_3O_4, and $CaCO_3$ have been mixed up in an agate mortar; the mixture has been first treated at 900 °C to decompose calcium carbonate. The resulting powder has been pressed (10 ton) into a rod and heated to 1160 °C under an O_2 atmosphere. Grinding, pressing, and firing steps have been repeated several times. In order to get an optimal oxygen content, two heat treatments under high oxygen pressure were performed after sintering: the first one at 900 °C with $p_{O_2}=200$ bars during 14 h; and the second at 475 °C with $p_{O_2}=150$ bars during 6 h. Prepared samples have been examined by x-ray powder diffraction using a Siemens D-5000 diffractometer. They have been found to be single phased and free from impurities.

Resistivity and magnetotransport measurements have been done using a commercial physical properties measurement system (PPMS, Quantum Design) in the temperature range $5<T<300$ K, by the four-probe method. Magnetization measurements have been done in a superconducting quantum interferometer device (SQUID, Quantum Design) using dc fields.

Neutron powder-diffraction (NPD) studies have been conducted at the Institute Max Von Laue-Paul Langevin (ILL, Grenoble) using diffractometers D20 ($\lambda=1.91$ Å, high-resolution mode) and D2B ($\lambda=1.594$ Å) at temperatures ranging from 10 K to RT. NPD diffractograms have been refined by the Rietveld method using FULLPROF suite of programs.[27]

III. RESULTS

Figure 1 shows the dc resistivity of $Pr_{0.50}Ca_{0.50}CoO_3$ measured by the four-probe method at zero field and under an applied field of 9 T in cooling-heating cycles. In accordance with previous works,[14,16,17] $\rho(T)$ shows a sudden drop (on heating) at $T_{MI}\approx 80$ K. Above T_{MI}, the electrical resistivity is low for a polycrystalline oxide (about 1 mΩ cm). This value is very similar to that measured in a single-crystal specimen,[21] and is comparable in magnitude with that found for $Pr_{0.50}Sr_{0.50}CoO_3$ and different $RBaCo_2O_{5+\delta}$ compounds.[23–26] In this temperature region ($T>T_{MI}$), resistivity scarcely depends on but clearly decreases with temperature and its behavior is thus semiconducting like rather than simply metallic (with rather low activation energy, 3.8 meV). This activation energy is smaller than the thermal k_BT energy, and an extrinsic origin related to local defects or domain boundaries cannot be ruled out. Below T_{MI}, resistivity suddenly increases showing a markedly insulating character. This transition presents a certain hysteresis in the cooling-heating cycle of about 4 K. The presence of a strong magnetic field (9 T) does not alter the behavior of the resistivity significantly. This field shifts down the T_{MI} by 5 K. Consequently, the magnetoresistance (inset of Fig. 1) presents a peak very near the MIT transition. Below this point ($T<T_{MI}$), resistance clearly decreases with the applied field, giving rise to a considerable magnetoresistance (20–40 %) but above this point ($T>T_{MI}$), the resistivity is hardly affected by the magnetic field and, in fact, the sign of the magnetoresistance depends on temperature. It becomes positive [$\rho(9\ \mathrm{T})>\rho(0\ \mathrm{T})$] above $T\approx 100$ K.

Figure 2(a) shows the magnetization of $Pr_{0.50}Ca_{0.50}CoO_3$ measured under 5 T of applied field on heating after zero-field-cool and field-cool processes. A sudden decrease in the magnetization takes place very near T_{MI}. The inverse of the dc susceptibility (χ) is also plotted in Fig. 2(a). Above 100 K $\chi^{-1}(T)$ follows a linear behavior rendering $\theta_C=65$ K and an effective paramagnetic moment $\mu_{eff}=4.43(2)\mu_B$/f.u. Assuming a paramagnetic contribution from Pr ions of $3.58\mu_B$/Pr, the estimated moment from Co ions is $3.64(3)\mu_B$/Co.

NPD patterns (on high-resolution D2B and D20 diffractometers) collected above 100 K can be very well refined using a single phase with space group *Pnma* ($a\approx c\approx a_p\times\sqrt{2}$; $b\approx 2a_p$). Below 100 K, NPD patterns clearly evidence the coexistence of two different phases, with quite similar cell

TABLE I. Structural details obtained by the Rietveld refinement of NPD data (D2B at RT and D2B-D20 at 100 and 10 K). In all cases the space group is *Pnma*. Co is at 4*b* position ($\frac{1}{2}$ 0 0), Pr/Ca and O1 at 4*c* positions (x $\frac{1}{4}$ y), and O2 at general 8*d* position. Agreement factors (for each pattern) and selected bond distances and angles are also listed.

				10 K	
		RT	100 K	LT phase	HT phase
a (Å)		5.3384(3)	5.3317(3)	5.3225(2)	5.3336(2)
b (Å)		7.5410(3)	7.5103(4)	7.4593(3)	7.5129(3)
c (Å)		5.3380(3)	5.3165(3)	5.2638(2)	5.3184(2)
V (Å^3)		214.89(2)	212.89(3)	208.98(2)	213.11(2)
wt %		100	100	92(1)	8(1)
Co	β	0.29(3)	0.33(3)	0.30(5)	0.33
Pr/Ca	x	0.0325(3)	0.0368(3)	0.0447(3)	0.0368
	z	0.0063(5)	−0.0072(6)	−0.0094(5)	−0.0072
	β	0.0325(3)	0.47(2)	0.50(3)	0.47
O1	x	0.4913(3)	0.4907(3)	0.4862(3)	0.4907
	z	0.0674(4)	0.0694(4)	0.0791(4)	0.0694
	β	0.85(2)	0.59(2)	0.50(2)	0.59
O2	x	0.2148(3)	0.2129(2)	0.2075(2)	0.2129
	y	−0.0341(1)	−0.0359(1)	−0.0402(2)	−0.0359
	z	0.2153(3)	0.2120(2)	0.2054(2)	0.2120
	β	0.69(1)	0.52(2)	0.59(2)	0.52
χ^2 (D2B)		7.0	5.3	5.6	
R_B (D2B)		3.77	3.46	3.29	5.28
χ^2 (D20)			5.8	5.9	
R_B (D20)			2.42	3.37	6.99
$d_{\text{Co-O1}}$ (Å)		1.920(1)	1.9141(8)	1.9121(5)	
$d_{\text{Co-O2}}$ (Å)		1.921(2)	1.920(2)	1.919(1)	
$d_{\text{Co-O2}}$ (Å)		1.925(2)	1.925(2)	1.927(1)	
$\langle d_{\text{Co-O}} \rangle$ (Å)		1.922(2)	1.920(2)	1.919(1)	
$\theta_{\text{Co-O1-Co}}$ (deg)		158.18(3)	157.57(3)	154.45(3)	
$\theta_{\text{Co-O2-Co}}$ (deg)		157.95(6)	156.54(6)	153.37(6)	
$\langle \theta_{\text{Co-O-Co}} \rangle$ (deg)		158.03(5)	156.88(5)	153.73(5)	
$\langle d_{\text{A-O}} \rangle^{\text{VIII}}$ (Å)		2.502(2)	2.484(2)	2.444(2)	
$\langle d_{\text{A-O}} \rangle^{\text{X}}$ (Å)		2.594(3)	2.581(2)	2.558(2)	

parameters. Both phases can be well described using the same *Pnma* space group. The phase that appears on cooling (LT phase) rapidly grows while the high-temperature phase (HT phase) decreases. This evolution stops at about 50 K and below this point a small portion of the sample remains in the HT phase. Table I displays the structural details obtained from the Rietveld refinement of neutron patterns (D2B data at RT and the joint refinement of D2B and D20 data at 100 and 10 K), together with the agreement factors and selected bond distances and angles. We have checked the oxygen content of our sample through the Rietveld refinement. Combining D2B and D20 data sets collected at 100 K, the refinement of oxygen occupancies does not indicate a decrease in the oxygen content from the nominal value. Low-temperature NPD diffractograms (10 K) show no evidence of long-range magnetic order. We have carefully examined the low-temperature diffractograms (D2B and D20), none of them presents evidences of superstructure peaks. Moreover, *Pnma* space group allows only one crystallographic position for Co. These two observations are against the appearance of charge order in this system.

Figure 3(a) shows the thermal evolution of the unit-cell volume of the coexisting phases (left axis) and the evolution of the amount of each phase (right axis). There is a large difference, around 2% (or 4 Å^3), between V of HT and LT phases, and this difference is nearly independent of temperature in the two phases region. Figure 3(b) shows the evolution in temperature of the lattice parameters. The reduction in V of the LT phase with respect to the HT phase comes from the decrease in, mainly, b and c lattice parameters while a does not change abruptly between the two phases. These data evidence the first-order nature of this phase transition.

Figure 4(a) presents the evolution in temperature of the average Co-O bond length across the MIT. It can be appre-

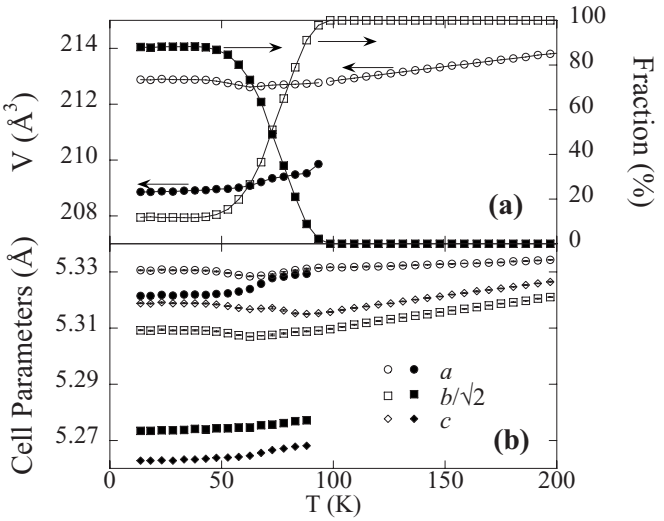

FIG. 3. Evolution with temperature of (a) unit-cell volume (left axis) and phase fraction (right axis) of coexisting cells, and (b) unit-cell parameters. Open and closed symbols stand for HT and LT phases, respectively.

ciated that this distance hardly changes during the electronic localization process at T_{MI}. This strongly supports that the large volume difference between LT and HT phases does not come from changes in the effective size of the CoO_6 units. Figure 4(b) plots the volume of the CoO_6 octahedra and the average Co-O-Co bond angles as a function of temperature. Consistently with the invariance of the mean Co-O bond distance, the remarkable decrease in the cell volume does not affect the volume of the octahedra. Consequently, it causes a strong bending of the Co-O-Co bond angles (of about 3° through the transition). This change in bond angle is huge, taking into account the narrow temperature interval where it takes place. From a steric point of view, this change (without a modification of the mean Co-O bond distance) necessarily requires strong atomic shifts within the coordination polyhedra associated to the *A* site (*A*-O sublattice). Figure 4(a) plots the average (Pr,Ca)-O (*A*-O) bond distance calculated up to eight neighbors. It evidences that there is a strong reduction (above 0.04 Å) in this bond distance at the phase transition. We can conclude that the structural details resulting from the refinement of the high-resolution diffraction data all point to the fact that the most remarkable changes across the transition take place at the *A* but not at the *B* position of this perovskite.

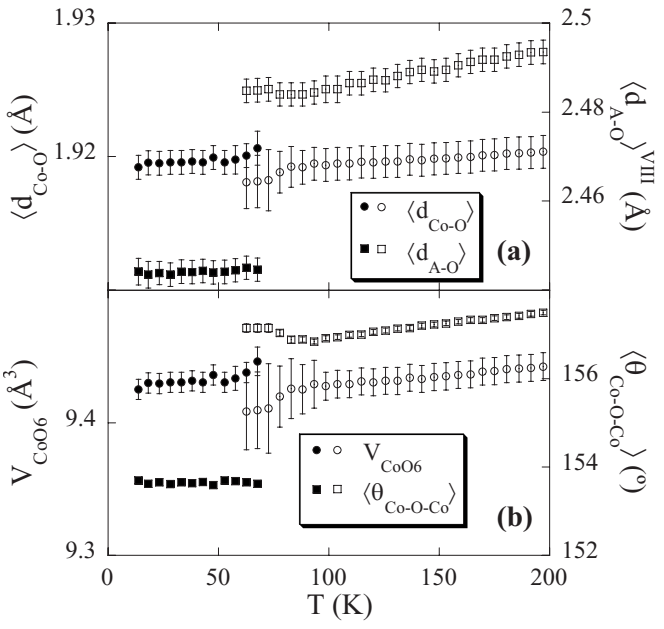

FIG. 4. Evolution with temperature of (a) average Co-O bond distance (left axis) and (Pr,Ca)-O (*A*-O) bond distance (right axis). Notice that the scale of the left axis is not the same as that of the right axis. (b) Evolution of the volume of the CoO_6 octahedra (right axis) and the average Co-O-Co bond angle (right axis). Open and closed symbols stand for HT and LT phases, respectively.

IV. DISCUSSION

It has been interpreted, as a widely accepted picture of the electronic changes taking place at the transition, that above T_{MI}, the electronic configuration of Co is $t_{2g}^5\sigma^{*0.5}$ while below this temperature, Co presents a mixture of Co(III) and Co(IV) (both in low spin state).[14–19] Besides, our measurements show that above 100 K, an applied field of 9 T scarcely affects the resistivity and, in fact, ρ slightly enlarges with the field. This demonstrates that the mobility of itinerant electrons does not depend on the magnetic arrangement of the core spins (t_{2g}^5). A first consequence of this observation is that the ferromagnetic interactions observed above T_{MI} (θ_C =+65 K) cannot be attributed to double exchange as main mechanism. Moreover, this observation challenges the conduction mechanism widely accepted above T_{MI}. Hund's-rule exchange coupling of e_g electrons with the spin of localized t_{2g} levels is expected to be weaker than, for instance, in magnetoresistive manganites. Nonetheless, from the electronic configuration $t_{2g}^5\sigma^{*0.5}$, a term $\propto\cos\theta/2$ (θ being the angle between neighboring core spins) in the hopping probability must be present. Looking at the experimental data shown in Fig. 1, we remark that a very strong field (9 T) does not drive to any reduction in the resistivity above T_{MI}. This contrasts with the behavior of metallic $Pr_{0.50}Sr_{0.50}CoO_3$ that shows a measurable magnetoresistance.[23] Concerning the insulating phase of $Pr_{0.50}Ca_{0.50}CoO_3$, Co ions are supposed to be in a LS state. Thus, the conduction would take place by hopping of t_{2g} electrons from nonmagnetic Co(III) (S=0) to Co(IV) ($S=\frac{1}{2}$). In that case (as the departing ion is nonmagnetic) the hopping probability could be (in first approximation) independent of the orientation of the moment of the arrival ion. In spite of this, magnetoresistance below T_{MI} takes values ranging between 20% and 40%.

The detailed structural information obtained as a function of temperature must be carefully analyzed in order to examine the mechanism behind this transition. As reported in previous works,[14,18,19] there is an important contraction of V on cooling across the transition. Spin-state transitions of Co ions are in fact accompanied by perceptible cell volume changes but these changes are driven by changes in Co size (deduced from the mean Co-O bond distance) induced by the new spin state.[10,11] According to literature, the difference in size be-

tween Co^{3+} in LS and IS or HS is around 0.016 Å and 0.04 Å, respectively.[10] Previous works take the change in V accompanying the MIT of $Pr_{0.50}Ca_{0.50}CoO_3$ as an evidence of the spin-state transition of Co. The more it must surprise that, according to Table I, the average Co-O bond distance (and the volume of CoO_6 octahedra) does not change across the transition. This is not expected in the current interpretation: on heating the spin-state transition would mainly consist of the promotion of a fraction of bonding (t_{2g}) electrons to an antibonding (e_g) state, which must be accompanied by a certain enlargement of the Co-O bond distances. The expected change in distance would be around 0.01 Å, greater than our error bars. In any case, it is clear that the driving force of the change in volume at the MIT is not a change in the size of Co ions. Instead, on cooling across the transition, there is a bending of the Co-O-Co bond angle by a very large amount: 3°. To illustrate the importance of this bond bending, we mention that it is comparable to that produced in $R_{0.5}Ca_{0.5}MnO_3$ perovskites series when going from R=Pr to the much smaller Sm (in this case, the change in V is −1.3%, at RT, and the change in the average Mn-O distance is 0.002 Å).[28] This comparison also allows to foresee that an important reduction in the space available for the cations at the A site of the perovskite must take place. This is confirmed by the abrupt reduction (on cooling) in the average A-O bond distance displayed in Fig. 4(a). This shortening is remarkably high (0.04 Å) and very unusual. It strongly points toward a relationship between the MIT and the behavior of the cations placed at this crystallographic position.

It is worth to compare the behavior of $Pr_{0.50}Ca_{0.50}CoO_3$ with that previously reported for different members of $RBaCo_2O_{5.50}$ family displaying a sudden spin-state transition concomitant with a MIT. R=Gd, Tb, and Pr members[11,29,30] display a change in volume across the spin-state transition of 0.3% (Tb) and 0.2% (Gd and Pr). Changes in size of octahedral Co are 0.038 Å (Tb), 0.01 Å (Gd), and 0.013 Å (Pr). Finally, the changes in A-site cations (coordination X) are 0.004 Å and 0.011 Å (for Ba and Tb, respectively); 0.006 Å and 0.007 Å (for Ba and Gd, respectively); and 0.007 Å (for both Ba and Pr). This comparison reinforces the fact that the volume change occurring at T_{MI} in $Pr_{0.50}Ca_{0.50}CoO_3$ is unusually large for a spin-state transition and must be ascribed to changes at the A site of the perovskite.

At this point, it is necessary to recall that the MIT transition has only been reported for $R_{0.50}Ca_{0.50}CoO_3$ with R=Pr. For the nearest lanthanides to Pr, R=La (bigger) or Nd (smaller), this transition does not take place.[15] Taking this fact into account, the sudden shortening of the A-O bond distance coinciding with the enhancement of the resistivity must be interpreted in terms of the occurrence of electronic changes in Pr ions. This shortening could be due to a hybridization of Pr 4f and O 2p orbitals as reported for $PrBa_2Cu_3O_{7-\delta}$. This type of hybridization is responsible for the suppression of superconductivity in 123 cuprates with Pr.[31] Hybridization of Bi 6s with O 2p orbitals has been shown to hinder the e_g electrons mobility in bismuth-based manganites thus inducing charge order at very high temperatures in these systems [up to 600 K (Ref. 32)]. It is worth mentioning that, in this last example, a certain expansion of MnO_6 octahedra is found as a consequence of this hybridization.[33,34] In the present case, the hybridization of Pr 4f levels with O 2p orbitals could provoke the electron localization and the enhancement of the resistivity.

Another possible interpretation arises if one takes into account that Pr can present 4+ valence (instead of 3+). According to our refinements, Pr has eight oxygen ions at a distance ranging between 2.34 and 2.62 Å and the other four oxygen ions placed at a distance very near or above 3 Å (above 2.94 Å). Thus, the coordination of Pr ions in this structure can be taken as VIII. According to Ref. 35, the radius of Pr^{4+} (with coordination VIII) is 0.166 Å smaller than Pr^{3+} (with coordination VIII). Thus, one would expect a difference in the A-O bond distance of 0.08 Å for a mixture of $Ca^{2+}Pr^{3+}$ and $Ca^{2+}Pr^{4+}$ (experimental shortening is 0.04 Å). Besides, the average Co-O bond distance reported for LS Co(III) is 1.925 Å, very similar to that find here and by other authors at low temperature [1.919(1) Å, as reported in Table I]. Thus, within this scenario, the sudden enhancement of the resistivity at T_{MI} would be due to a charge transfer from A sublattice (due to partial Pr^{3+} to Pr^{4+} conversion) to B sublattice of the perovskite that would transform a fraction of Co^{4+} into Co^{3+} ions. According to standard bond-valence-sum calculations, the change in valence of Pr is $0.6e^-$ while an estimation based on the average radius renders a change near $0.5e^-$. This change would fill the band and hinder the charge movement. Elucidating between these (or other) possibilities, as well as understanding the behavior of the magnetoresistance will require further research efforts.

Furthermore, with the aim of obtaining an independent confirmation of our conclusions about the key role of Pr atoms for the MIT, we prepared $La_{1/6}Nd_{1/3}Ca_{0.5}CoO_3$. This specific composition was chosen because Pr atoms are not present but the average ionic radius at A site is identical to $Pr_{0.5}Ca_{0.5}CoO_3$.[35] The magnetization of $La_{1/6}Nd_{1/3}Ca_{0.5}CoO_3$ is shown in Fig. 2(b) measured under the same conditions as that in Fig. 2(a) for $Pr_{0.5}Ca_{0.5}CoO_3$. In addition to the paramagnetic moment of Nd, a clear ferromagnetic order of Co moments is observed below $T_C \approx 125$ K. But the most remarkable is that the sharp drop of magnetization distinctive of the MIT in $(Pr,Ca)CoO_3$ cobaltites[16] is absent. Instead of a drop in the magnetization this cobaltite (with the same doping and expected ⟨Co-O-Co⟩ distortion than $Pr_{0.5}Ca_{0.5}CoO_3$) exhibits a ferromagnetic order of Co moments. The figure shows the lack of the MIT and a FM-ordered state in absence of Pr atoms. Therefore, Fig. 2(b) independently confirms our conclusion that the MIT and the associated volume contraction is due to electronic changes in Pr. As mentioned before, from neutron-diffraction data, we have inferred a change in the Pr valence across the transition of between $0.5e^-$ and $0.6e^-$.

V. SUMMARY

In summary, by means of resistivity, magnetotransport, magnetic measurements, and high-resolution neutron powder diffraction and thermodiffraction, we have investigated the metal-insulator transition in $Pr_{0.50}Ca_{0.50}CoO_{3-\gamma}$ (with $\gamma \approx 0$). We have tried to examine our results in the framework of the

picture drawn in previous works, that attribute the origin of this MIT to a change from LS states of Co^{3+} (t_{2g}^6) and Co^{4+} (t_{2g}^5) below T_{MI}, to $t_{2g}^5(\sigma^*)^{0.5}$ state above T_{MI}. We have found that the behavior of the magnetoresistance and of the Co-O bond distance (or, equivalently, the volume of the CoO_6 octahedra) is in contradiction with this simple picture. On the other hand, a very remarkable shortening in the (Pr,Ca)-O bond distance during the MIT takes place that forces a huge bending of the Co-O-Co bond angles. Consequently, these observations make us to conclude that the volume contraction at MIT is due to a sudden modification in the effective ionic radius of the *A*-site cations of the perovskite (presumably Pr ions), instead of to a change in the size of Co ions. The key role of Pr ions has been discussed and two possible situations considered: a localization of itinerant electrons due to hybridization of Pr 4*f* with O 2*p* orbitals and a possible partial charge transfer from *A* to *B* sites ($Pr^{3+}/Co^{4+} \rightarrow Pr^{4+}/Co^{3+}$) in this perovskite below T_{MI}. The absence of this transition in $La_{1/6}Nd_{1/3}Ca_{0.5}CoO_3$ also confirms the active role of Pr ions.

ACKNOWLEDGMENTS

Financial support from MICINN (Spanish government) under Projects No. MAT2006-11080-C02-02 and No. NANOSELECT CSD2007-00041, Generalitat de Catalunya (Grant No. 2005-GRQ-00509) and FAME European Network of Excellence is acknowledged. We thank Institute Laue Langevin for the provision of beamtime.

[1] Z. Shao and S. M. Haile, Nature (London) **431**, 170 (2004).
[2] Y. Wang, N. S. Rogado, R. J. Cava, and N. P. Ong, Nature (London) **423**, 425 (2003).
[3] W. Kobayashi, S. Ishiwata, I. Terasaki, M. Takano, I. Grigoraviciute, H. Yamauchi, and M. Karppinen, Phys. Rev. B **72**, 104408 (2005).
[4] S. Yáñez-Vilar, A. Castro-Couceiro, B. Rivas-Murias, A. Fondado, J. Mira, J. Rivas, and M. A. Señarís-Rodríguez, Z. Anorg. Allg. Chem. **631**, 2265 (2005).
[5] C. Martin, A. Maignan, D. Pelloquin, N. Nguyen, and B. Raveau, Appl. Phys. Lett. **71**, 1421 (1997).
[6] I. O. Troyanchuk, N. V. Kasper, D. D. Khalyavin, H. Szymczak, R. Szymczak, and M. Baran, Phys. Rev. Lett. **80**, 3380 (1998); Phys. Rev. B **58**, 2418 (1998).
[7] A. Maignan, V. Caignaert, B. Raveau, D. Khomskii, and G. Sawatzky, Phys. Rev. Lett. **93**, 026401 (2004).
[8] K. Takada, H. Sakurai, E. Takyama-Muromachi, F. Izumi, R. A. Dilanian, and T. Sasaki, Nature (London) **422**, 53 (2003).
[9] M. A. Señarís-Rodríguez and J. B. Goodenough, J. Solid State Chem. **116**, 224 (1995).
[10] P. G. Radaelli and S.-W. Cheong, Phys. Rev. B **66**, 094408 (2002).
[11] C. Frontera, J. L. García-Muñoz, A. Llobet, and M. A. G. Aranda, Phys. Rev. B **65**, 180405(R) (2002).
[12] I. A. Zaliznyak, J. M. Tranquada, R. Erwin, and Y. Moritomo, Phys. Rev. B **64**, 195117 (2001); N. Sakiyama, I. A. Zaliznyak, S.-H. Lee, Y. Mitsui, and H. Yoshizawa, *ibid.* **78**, 180406(R) (2008).
[13] K. Knížek, P. Novák, and Z. Jirák, Phys. Rev. B **71**, 054420 (2005).
[14] S. Tsubouchi, T. Kyômen, M. Itoh, P. Ganguly, M. Oguni, Y. Shimojo, Y. Morii, and Y. Ishii, Phys. Rev. B **66**, 052418 (2002).
[15] H. Masuda, T. Fujita, T. Miyashita, M. Soda, Y. Yasui, Y. Kobayashi, and M. Sato, J. Phys. Soc. Jpn. **72**, 873 (2003).
[16] S. Tsubouchi, T. Kyômen, M. Itoh, and M. Oguni, Phys. Rev. B **69**, 144406 (2004).
[17] T. Fujita, T. Miyashita, Y. Yasui, Y. Kobayashi, M. Sato, E. Nishibori, M. Sakata, Y. Shimojo, N. Igawa, Y. Ishii, K. Kakurai, T. Adachi, Y. Ohishi, and M. Takata, J. Phys. Soc. Jpn. **73**, 1987 (2004).
[18] A. Chichev, J. Hejtmánek, Z. Jirák, K. Knížek, M. Maryško, M. Dlouhá, and S. Vratislav, J. Magn. Magn. Mater. **316**, e728 (2007).
[19] A. Chichev, M. Dlouhá, S. Vratislav, J. Hejtmánek, Z. Jirák, K. Knížek, and M. Maryško, Z. Kristallogr. Suppl. **26**, 435 (2007).
[20] I. G. Deac, R. Tetean, D. Andreica, and E. Burzo, IEEE Trans. Magn. **44**, 2922 (2008).
[21] J. Zhou, P. Zheng, and N. L. Wang, J. Phys.: Condens. Matter **20**, 055222 (2008).
[22] P. Tong, Y. Wu, B. Kim, D. Kwon, J. M. S. Park, and B. G. Kim, J. Phys. Soc. Jpn. **78**, 034702 (2009).
[23] R. Mahendiran and P. Schiffer, Phys. Rev. B **68**, 024427 (2003).
[24] M. A. Señarís-Rodríguez and J. B. Goodenough, J. Solid State Chem. **118**, 323 (1995).
[25] K. Yoshii, H. Abe, and A. Nakamura, Mater. Res. Bull. **36**, 1447 (2001).
[26] R. Ganguly, A. Maignan, C. Martin, M. Hervieu, and B. Raveau, J. Phys.: Condens. Matter **14**, 8595 (2002).
[27] J. Rodríguez-Carvajal, Physica B **192**, 55 (1993).
[28] P. M. Woodward, T. Vogt, D. E. Cox, A. Arulraj, C. N. R. Rao, P. Karen, and A. K. Cheetham, Chem. Mater. **10**, 3652 (1998).
[29] H. Kusuya, A. Machida, Y. Moritomo, K. Kato, E. Nishibori, M. Takata, M. Sakata, and A. Nakamura, J. Phys. Soc. Jpn. **70**, 3577 (2001).
[30] C. Frontera, J. L. García-Muñoz, A. E. Carrillo, M. A. G. Aranda, I. Margiolaki, and A. Caneiro, Phys. Rev. B **74**, 054406 (2006).
[31] R. Fehrenbacher and T. M. Rice, Phys. Rev. Lett. **70**, 3471 (1993); S. K. Malik, S. M. Pattalwar, C. V. Tomy, R. Prasad, N. C. Soni, and K. Adhikary, Phys. Rev. B **46**, 524 (1992).
[32] C. Frontera, J. L. García-Muñoz, M. A. G. Aranda, M. Hervieu, C. Ritter, Ll. Mañosa, X. G. Capdevila, and A. Calleja, Phys. Rev. B **68**, 134408 (2003); J. L. García-Muñoz, C. Frontera, M. Respaud, M. Giot, C. Ritter, and X. G. Capdevila, *ibid.* **72**, 054432 (2005).
[33] J. L. García-Muñoz, C. Frontera, M. A. G. Aranda, A. Llobet, and C. Ritter, Phys. Rev. B **63**, 064415 (2001).
[34] N. A. Hill and K. M. Rabe, Phys. Rev. B **59**, 8759 (1999).
[35] R. D. Shannon, Acta Crystallogr., Sect. A: Cryst. Phys., Diffr., Theor. Gen. Crystallogr. **32**, 751 (1976).